water

MDPI

Article

The Impact of Extreme Precipitation on Soil Moisture Transport in Apple Orchards of Varying Ages on the Loess Plateau

Jialiang Huang [1,2], Yi Hua [3], Yuqing Zhang [1,2], Wei Xu [1,2], Linyun Gu [1,2], Yu Tian [1,2], Yi Wu [1,2,*], Quan Long [1,2], Haoyan Wei [4] and Min Li [4]

[1] Sichuan Academy of Eco-Environmental Sciences, Chengdu 610041, China
[2] Sichuan Province Engineering Technology Research Center of Emerging Contaminants Treatment and Environmental Health, Chengdu 610041, China
[3] Sichuan Academy of Water Conservancy, Chengdu 610041, China
[4] Institute of Water-Saving Agriculture in Arid Areas of China, Northwest A&F University, Yangling 712100, China
* Correspondence: yeen.wu@gmail.com

Abstract: The long-term cultivation of apple trees with deep root systems can significantly deplete moisture from the deep soil layers, while extreme rainfall events can rapidly replenish this moisture. Therefore, it is of great academic significance to investigate the influence of extreme precipitation on soil water dynamics in apple orchards of varying ages. This study was conducted on agricultural land and apple orchards of 12 years, 15 years, 19 years and 22 years (12 y, 15 y, 19 y and 22 y) to examine the impact of extreme precipitation on soil moisture transport. Soil moisture content and hydrogen and oxygen isotope (^{2}H, ^{18}O and ^{3}H) data were collected before (October 2020 and May 2021) and after the extreme precipitation event (May 2022). This comprehensive analysis focuses on two aspects: soil moisture distribution and soil water recharge. The following main conclusions were drawn: (1) Extreme precipitation significantly enhanced deep soil water recharge in apple orchards: the depths of soil water supply for apple orchards of 12 y, 15 y, 19 y and 22 y were recorded as 282 mm, 180 mm, 448 mm and 269 mm, respectively. Correspondingly, the recharge depths were measured at approximately 12, 10, 10 and 7 m, respectively. It was observed that the recharge depth decreased with increasing age of the orchard. (2) Extreme precipitation did not have a significant impact on the values of $\delta^{2}H$ and $\delta^{18}O$ of deep soil moisture due to a limited infiltration depth through the piston flow mechanism (the maximum infiltration depth being around 3 m). (3) In agricultural land as well as apple orchards of 12 y, 15 y and 22 y in 2020, the tritium peak occurred at soil depths of 7.2, 6.9, 6.7 and 5.7 mm, respectively; in 2022, the corresponding values increased to 7.9, 8.7, 6.7 and 5.9 mm, respectively. This indicates that planting apple trees hindered the transport of soil moisture. The peak concentration of tritium in both agricultural land and different-aged apple orchards decreased after experiencing extreme precipitation. The findings will provide a scientific basis for water resource management and efforts toward ecological restoration on the Loess Plateau.

Keywords: soil moisture; extreme precipitation; apple orchards; hydrogen and oxygen isotope

check for updates

Citation: Huang, J.; Hua, Y.; Zhang, Y.; Xu, W.; Gu, L.; Tian, Y.; Wu, Y.; Long, Q.; Wei, H.; Li, M. The Impact of Extreme Precipitation on Soil Moisture Transport in Apple Orchards of Varying Ages on the Loess Plateau. *Water* **2024**, *16*, 3322. https://doi.org/10.3390/w16223322

Received: 17 October 2024
Revised: 15 November 2024
Accepted: 16 November 2024
Published: 19 November 2024

Copyright: © 2024 by the authors. Licensee MDPI, Basel, Switzerland. This article is an open access article distributed under the terms and conditions of the Creative Commons Attribution (CC BY) license (https://creativecommons.org/licenses/by/4.0/).

1. Introduction

Soil moisture serves as a crucial resource for plant growth and underpins ecosystem health, particularly in arid and semi-arid regions [1–3]. The Loess Plateau, located in China, is a typical arid and semi-arid region where the temporal and spatial dynamics of soil moisture are profoundly influenced by topography and precipitation patterns [4–6]. In recent years, many studies have focused on the temporal and spatial dynamics of soil moisture on the Loess Plateau [7–10]. Li et al. verified that topography mainly affects the soil moisture of the shallow soil layers, with the soil moisture of the deep layers being mainly affected by vegetation [7]. Xu et al. found that soil moisture levels varied by land

type, with bare land exhibiting the highest moisture content, followed by grassland and forestland [11].

In the past two decades, stable isotope technology has experienced increasing application in various hydrogeological fields [12]. As a natural tracer, stable isotopes can provide valuable insights into soil moisture flux, including data on evaporation, transpiration and infiltration, which are typically challenging to obtain using alternative techniques [13]. Han et al. analyzed the characteristics of stable hydrogen and oxygen isotopes of soil moisture in these different land use types at different soil depths; the results show that along the soil depth in forest land, the hydrogen isotope increased first and then decreased, while increased in the end, and the maximum appeared in 80–100 cm [12]. Du investigated the hydrogen and oxygen isotopic compositions of soil water and analyzed the influence of land use, indicating that the stable isotope values in shallow (<100 cm depth) soil water and deep (>200 cm depth) soil water were low [14].

Extreme precipitation events can significantly enhance the recharge of deep soil moisture [15]. In the semi-arid loess region, the results show that in extreme precipitation years, the soil water recharge of shrubs and grasslands mainly occurs in the 0–2 m soil layer, while that of cultivated land and farmland can reach the 4 m deep soil layer [16]. The soil water storage increased by 54–85% in relatively abundant water scenarios compared with scarce water scenarios on the Loess Plateau [5]. However, currently, there is a scarcity of studies on the impact of extreme precipitation on soil water recharge, particularly in the context of natural extreme rainfall conditions. Therefore, it is imperative to investigate the depth and magnitude of extreme precipitation in relation to deep soil water recharge. The replenishment of groundwater through precipitation can be achieved via piston flow and preferential flow mechanisms [17]. Although some scholars have examined the groundwater recharge mode in loess tablelands, there remains controversy surrounding the dominant mechanism [18]. Certain studies have indicated that the piston flow serves as the primary mode for groundwater replenishment [19], with preferential flow generation relying on a specific threshold level of precipitation [20]; thus, extreme precipitation events offer an excellent opportunity to validate this perspective.

The purpose of this study was to study the changes in soil moisture content in apple orchards at different depths before and after extreme precipitation events and to assess the ecohydrological processes associated with extreme rainfall events and apple tree planting.

2. Materials and Methods

2.1. Study Site Description

The study area is located in Changwu County of Shaanxi Province (107°41′ E, 35°14′ N) in the central and southern part of the Loess Plateau (Figure 1), with an average annual temperature of 9.2 °C and annual average precipitation of 573 mm (from 1994 to 2017), belonging to a typical warm temperate sub-humid continental monsoon climate. The average altitude of the local area is about 1230 m, the soil layer is deep, and the groundwater depth is mostly between 30 and 100 m [21]. The parent material is mostly Malan loess; the dry bulk density, pH value, organic matter content and total nitrogen content of the soil are 1.44 g/cm^3, 8.1, 13.3 g/kg, and 0.82 g/kg, respectively. The permanent wilting coefficient and field water capacity in the study area were 7.46% ± 0.65% and 21.16% ± 0.86%, respectively [22].

According to the *China Statistical Yearbook*, the Loess Plateau is a crucial ecoregion for apple production, with 1.22 million hectares of apple orchards, representing 58% of China's planted area and 25% of the world's total. Since the 1990s, the Changwu Yuan region has actively expanded its apple industry, resulting in 16,733 hectares of apple trees and an output of 338,000 tons by 2020 [23].



Figure 1. Geographical location of the study area and distribution of each sampling point.

2.2. Experiment Design

In this experiment, apple orchards of varying ages (12 y, 15 y, 19 y and 22 y) in Changwu Yuan were selected as the main research objects through the method of spatial-temporal exchange. Detailed information can be found in Table 1. The apple varieties were all *Malus pumila* Mill, and the field management mode was the same. Meanwhile, agricultural land was sampled as a control.

Table 1. Apple orchard planting year, stand age, classification and geographical distribution.

Land Types	Planting Year	Stand Age	Period	Latitude	Longitude
Agricultural land	\	\	\	107°41′7.96″	35°14′52.75″
Apple orchard	2008	12 years	Full bearing	107°41′05.88″	35°14′58.72″
	2005	15 years	Full bearing	107°41′09.01″	35°14′52.18″
	2001	19 years	Senescence	107°40′46.74″	35°14′34.12″
	1998	22 years	Senescence	107°41′03.00″	35°14′08.82″

2.3. Data Acquisition

2.3.1. Meteorological Data Acquisition

The meteorological data of the temperature, precipitation, relative humidity and other factors were collected from the China Meteorological Data Network (https://data.cma.cn/) accessed on 10 July 2021.

2.3.2. Sample Collection

(1) Soil sample collection

In order to study the effects of extreme precipitation on soil water transport in apple orchards of varying ages in Changwu Yuan, soil samples were collected before extreme precipitation (October 2020, May 2021) and after extreme precipitation (May 2022). Among them, the last rainy season just ended in October 2020, while the current rainy season had not yet started in May 2021. Therefore, the recharge of soil water from October 2020 to May 2022 mainly comes from the rainy season precipitation in 2021, which is the extreme precipitation studied in this paper.

In October 2020, the sampling depth was 15 m, and in May 2022, the sampling depth reached the maximum recharge depth of extreme precipitation (Table 2). In addition, considering that the shallow soil moisture and soil water isotope will be affected by seasonal factors, this study conducted another sampling in May 2021 to ensure that May 2021 and May 2022 were in the same season, experiencing a complete dry season and rainy season in one year. Since only shallow soil is affected by seasonal factors, the sampling depth was selected to be 6 m.

Table 2. Sampling depth of agricultural land and apple orchards of varying ages.

Land Types	Sampling Depth (m)		
	October 2020	May 2021	May 2021
Agricultural land	0~15	\	0~15
Apple orchards of 12 y	0~15	0~6	0~12
Apple orchards of 15 y	0~15	0~6	0~10
Apple orchards of 19 y	0~15	0~6	0~10
Apple orchards of 22 y	0~15	0~6	0~8

Soil samples were collected in the middle of four trees with good growth and representing the average growth level of the whole orchard. A soil drill was used to drill fresh soil samples every 20 cm. Part of the fresh soil sample was placed into an aluminum box for soil moisture determination, and part was sealed into a plastic bottle and brought back to the room for refrigeration (−20 °C) for soil moisture extraction and later water isotope determination.

(2) Precipitation sample collection

Precipitation is one of the important sources of soil water recharge and plant water consumption in the study area [24]. In this study, precipitation isotope observation and collection points (35°14′ N,107°4′ E, 1200 m) were set up in Changwu Yuan to continuously collect the local precipitation events from 2015 to 2021 and determine the stable isotope composition of hydrogen and oxygen. In order to reduce the influence of evaporation fractionation on the isotopic composition of precipitation, an evaporation-proof precipitation collection device (Patent No: CN201620301350.6) was used to collect atmospheric precipitation. The device can provide a reliable guarantee for the accuracy of the precipitation isotope data collected in this study [24]. The collected water samples were returned to the laboratory in time for the determination of the stable isotope composition of hydrogen and oxygen.

(3) Leaf area index collection

A canopy analyzer (Li-2200C, Li-cor, Lincoln, NE, USA) was used to determine the leaf area index (LAI) of the apple orchards. Six apple trees were randomly selected to measure the radiative permeability density in the upper and lower parts of the canopy, and the leaf area index was estimated using the conversion model [7]. Each point needs to survey the upper part of the canopy once, survey the lower part four times, and correct for light scattering [25]. In order to avoid the influence of changes in the light environment on the measurement results, the LAI was determined in the early morning or evening when the sky scattering was uniform.

2.3.3. Soil Physical Properties Determination

(1) Soil bulk density

By weighing the mass of the ring knife before and after taking the soil, the quality of fresh soil in the ring knife was calculated, and the dry soil mass was converted by using the soil mass water content at the corresponding depth [26]. Finally, the soil bulk density (ρ_b) of the layer was converted by dividing the ring knife volume (100 cm^3). The calculation formula is as follows:

$$\rho_b = m_d / v \quad (1)$$

where ρ_b is the soil bulk density (g·cm^{-3}); m_d is the drying soil weight (g); v is the soil volume (cm^3).

(2) Soil texture classification

The soil texture was determined by the pipe straw method after the soil samples were air-dried, ground and sifted through a 2 mm screen. According to the USDA classification standard, soil particles were divided into clay (<0.002 mm), silt (0.002~0.05 mm) and sand (0.05~2 mm) [27].

(3) Soil moisture content

After subjecting the wet soil sample to a baking process in an oven set at 105 °C for a minimum duration of 24 h, until it attained a consistent weight, the determination of the soil moisture contentwas achieved by calculating the ratio between the water loss and the mass of dry soil [28]. Furthermore, utilization of the measured bulk density data at various depths facilitated the conversion to the volumetric soil moisture content at those specific depths. The formula employed for computing the volumetric soil moisture content is as follows:

$$\theta = \frac{(m_w - m_d)}{m_d} \times \rho_b \times 100\% \quad (2)$$

where θ is the volumetric soil moisture content (%); m_w is the wet soil weight (g); m_d is the drying soil weight (g); ρ_b is the soil bulk density (g·cm^{-3}).

2.3.4. Hydrogen and Oxygen Isotope Determination

Hydrogen and oxygen isotope determination of the soil water was divided into two parts: soil moisture extraction and isotope determination. Soil moisture was extracted from the soil samples by a cryogenic vacuum extraction system in the tracer hydrology Laboratory of China Arid Regions Water-Saving Agricultural Research Institute, Northwest A&F University. When utilizing the extraction device, the sample is initially cryogenically frozen using liquid nitrogen and subsequently subjected to vacuum heating to ensure complete removal of moisture from the sample. To guarantee sufficient extraction of soil moisture, both the extraction and collection efficiencies are calculated. If both efficiencies are $\geq$ 99%, the extraction is deemed satisfactory; otherwise, repeated extractions of the soil sample will be conducted [29]. Following completion of the experiment, the extracted soil moisture samples were sealed in 25 mL glass bottles and refrigerated at 4 °C in order to prevent evaporation and isotopic fractionation.

The determination of ^{2}H and ^{18}O in the precipitation and soil moisture samples was conducted at the Tracer Hydrology Laboratory of China Arid Regions Water-Saving Agricultural Research Institute, Northwest A&F University. The liquid water laser isotope analyzer was employed as the testing instrument. The hydrogen and oxygen stable isotopes were measured with an accuracy of $\pm$1% and $\pm$0.2%, respectively. The isotope expression for the analyzed water sample is as follows:

$$\delta = \frac{R_{Sample} - R_{Stand}}{R_{Stand}} \times 1000 \quad (3)$$

where R_{Sample} and R_{Stand} are the ratio of ^{2}H/^{1}H (or ^{18}O/^{16}O) between the sample to be tested and the reference standard water, respectively. The reference standard water is Weiye seawater.

The determination and analysis of tritium in the soil moisture samples were completed in the tracer Hydrology Laboratory of China Arid Regions Water-Saving Agriculture Research Institute, Northwest A&F University, using an ultra-low background liquid scintillation counter (Figures 2 and 3). About 8 mL of the extracted moisture sample was mixed with 12 mL of the scintillation solution and then left in the dark for 24 h. Tritium's activity was measured with an ultra-low-background liquid scintillation counter over a 500 min mean count-per-minute (CPM) period. After correcting for background noise with a tritium-free sample, the net CPM was then converted into tritium units [30]. The standard

error of the liquid scintillation counter is about 5 TU, and the detection limit is 3.29 times the measurement error, which is 16.5 TU.



Figure 2. Liquid water laser isotope analyzer.



Figure 3. Low background liquid scintillation counter.

2.4. Calculation Method

2.4.1. Soil Water Storage and Available Soil Water Deficit

To quantitatively describe the effects of extreme rainfall on soil water, soil water storage (*SWS*) and soil water deficit (*SWD*) were used. Its calculation formula is as follows:

$$SWS = SW \times \rho_b \times h \quad (4)$$

$$WD = (WF \times \rho_b \times h) - SWS \quad (5)$$

where *SWS* is the soil water storage (mm). ρ_b is the soil bulk density (g·cm^{-3}). *SWD* is the soil water deficit (mm). h is the depth of the soil layer (mm); *WF* is the field capacity (%).

2.4.2. Convection Diffusion Equation

On the Loess Plateau, most of the infiltration water moves in the form of piston flow during the infiltration process, and the new water pushes the old water down and down. As a result, the old water is below, and the new water is above, which lays a foundation for the application of the isotope methods to study groundwater recharge [31].

Tritium can form part of the water molecules, so it can be used to trace the movement of groundwater. The artificial tritium produced by nuclear tests is oxidized to form tritium water, which falls to the surface in the form of atmospheric precipitation and spreads throughout the atmosphere, playing a marker role in the modern environment. Several large nuclear explosions in history correspond to several peaks of tritium concentration in water, the largest of which was in 1963, which provides a reliable basis for the study of

groundwater migration [32,33]. When determining the location of the tritium peak, the convective dispersion equation was used to fit the soil tritium distribution:

$$C(z,t) = \frac{M_0 z}{2J_w\sqrt{\pi D t^3}} exp\left(-\frac{(z-z_0)^2}{2Dt}\right) \quad (6)$$

where $C(z, t)$ is the concentration equation of the tracer at depth z and time t; z_0 is the average depth (mm); D is the dispersion coefficient.

2.4.3. Lc-Excess

The isotopic composition of soil moisture is influenced by the combined effects of evaporation enrichment and precipitation infiltration, while water absorption by plant roots does not contribute to the enrichment of soil moisture isotopes [34]. Evaporative fractionation results in increased isotope values, whereas non-fractionating inputs from precipitation lead to decreased isotope values. Therefore, variations in the values of soil moisture isotopes can reflect the intensity and extent of interaction between surface evaporation and precipitation infiltration. Linear excess is quantified by measuring the distance between the ^{2}H and ^{18}O components of soil water and the local atmospheric precipitation line. The expression can be formulated as follows:

$$\text{lc-excess} = \delta^2 H - \text{a}\delta^{18}\text{O} - \text{b} \quad (7)$$

where a and b represent the slope and intercept of the local meteorological water line (LMWL), respectively. According to the definition, the lc-excess of the precipitation isotope is 0, indicating that evaporation has not occurred. The lc-excess value of the water samples after evaporation is usually negative, and the lower the negative value is, the more intense the evaporation degree is characterized [30,35]. Therefore, the vertical variation of the lc-excess value in the soil profile indicates the alternating variations in precipitation infiltration and soil evaporation, and the deep and shallow soil layers can be divided accordingly.

3. Results and Analysis

3.1. Interannual Variation Characteristics of Autumn Rainfall and Division of Extreme Precipitation Years

3.1.1. Interannual Variation Characteristics of Autumn Rainfall

The monthly precipitation in Changwu County from 2015 to 2021 is illustrated in Figure 4. In accordance with astronomical division, the seasons were defined as follows: spring (March to May), summer (June to August), autumn (September to November) and winter (December to February). The total annual precipitation recorded in 2021 reached a value of 764.8 mm, occurring, on average, for about 107 days throughout the year. Notably, six instances of extreme precipitation events exceeding both a duration of 24 h and an amount surpassing 30 mm were observed: 15 July (70.4 mm), 18 September (34.6 mm), 22 September (34.2 mm), 25 September (30.4 mm), 3 October (60.8 mm) and 6 October (36 mm). Furthermore, it is worth mentioning that during September, October and November, respectively, the cumulative rainfall was measured at levels of 226.8, 175.4 and 3 mm. These three months accounted for approximately 53% of the overall annual precipitation.

Figure 5 shows the proportion of autumn rainfall, annual rainfall and the proportion of autumn rainfall to annual rainfall from 2015 to 2021. It can be seen that the annual rainfall difference between 2015 and 2020 is not large, basically between 500 and 750 mm. However, there was a large gap between the autumn rainfall in varying years: the autumn rainfall from 2015 and 2020 was between 100 and 200 mm, accounting for 15% to 30% of the annual rainfall, while the autumn rainfall in 2021 was as high as 400 mm, accounting for more than 50% of the annual rainfall.

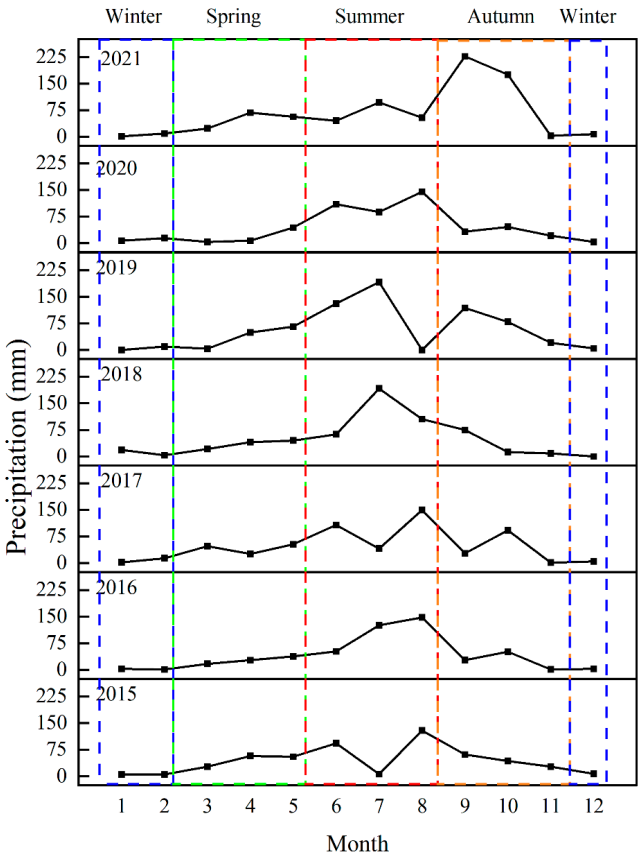


Figure 4. The monthly precipitation from 2015 to 2021.

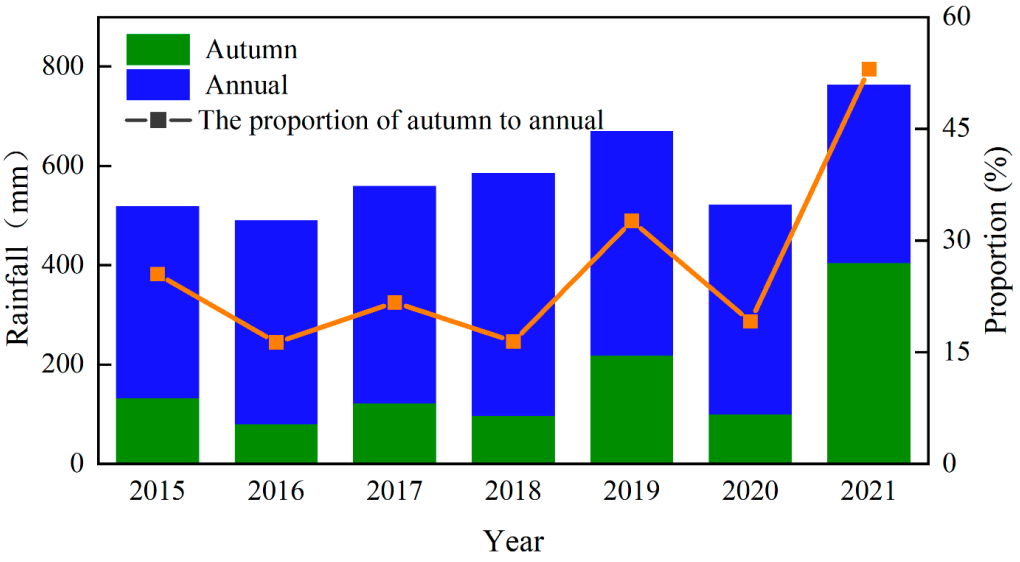


Figure 5. Autumn rainfall, annual rainfall and proportion from 2015 to 2021.

3.1.2. Division of Extreme Precipitation Years

In order to further analyze the changes in autumn rainfall, this study comprehensively considered the precipitation and the precipitation days while using the autumn rain index (ARI) to divide the ordinary precipitation year and the extreme precipitation year in the study area (Table 3). According to the variation range of the ARI from 2015 to 2021 (the average value ± standard deviation = 8.9 ± 5.6), the ARI from 2015 to 2020 was within the variation range, while the ARI in 2021 was outside the variation range. Therefore, the

autumn rainfall can be divided into an ordinary precipitation year (2015–2020) and extreme precipitation year (2021).

Table 3. Autumn rain index and classification of autumn rain types from 2015 to 2021.

Year	Precipitation Days (d)	ARI	Type
2015	31	7.9	Ordinary precipitation year
2016	29	4.7	Ordinary precipitation year
2017	32	6.9	Ordinary precipitation year
2018	32	5.3	Ordinary precipitation year
2019	28	9.1	Ordinary precipitation year
2020	36	6.9	Ordinary precipitation year
2021	40	21.2	Extremely precipitation year
Average value	32.6	8.9	
Standard deviation	4.2	5.6	

3.2. Effects of Extreme Precipitation on Distribution of Soil Moisture Characteristics in Apple Orchards of Varying Ages

3.2.1. Effects of Extreme Precipitation on Soil Moisture Content in Apple Orchards of Varying Ages

Figure 6 shows the distribution of the soil moisture content with depth in agricultural land and orchards of varying ages in 2020, 2021 and 2022, respectively. It can be seen that there was no significant change in the soil moisture content curve of agricultural land before extreme precipitation (2020) and after extreme precipitation (2022), but in apple orchards of varying ages, the soil moisture content curve changed significantly before extreme precipitation (2020) and after extreme precipitation (2022). The soil moisture content of the shallow soil layer after extreme precipitation was less than that before the extreme precipitation; the soil moisture content of the deep soil layer after extreme precipitation was greater than that before extreme precipitation. The results showed that extreme precipitation could greatly supplement the soil moisture in the shallow soil layer in apple orchards. There was no effect on the soil moisture in agricultural land. The decrease in soil moisture in the shallow layer of the orchard was mainly affected by the evaporation condition in the recent period before sampling.

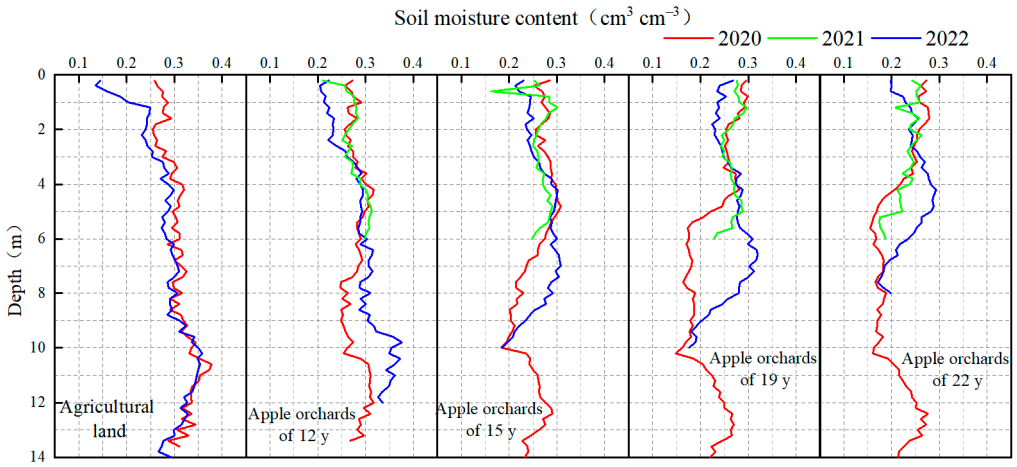


Figure 6. Distribution of soil moisture content with depth in agricultural land and orchards of varying ages in 2020, 2021 and 2022.

It can be seen that the shallow soil moisture content was greater before extreme precipitation than after extreme precipitation, and the soil moisture content of the deep

soil layer mainly reflected the influence of precipitation and evapotranspiration in the previous dry season. Below this depth, the soil water content begins to increase after extreme precipitation, so the research scope of the soil water being recharged by extreme precipitation below 4 m was taken as the research scope.

3.2.2. Effects of Extreme Precipitation on δ^2H and $\delta^{18}O$ of Soil Moisture in Apple Orchards of Varying Ages

The distribution of the δ^2H of soil moisture with a soil depth in agricultural land and apple orchards of varying ages in 2020, 2021, and 2022 is illustrated in Figure 7. It can be observed that in 2020, the δ^2H in apple orchards increased approximately with an increasing soil depth within the range of 0–3 m, while the fluctuation amplitude and depth decreased as the age increased; in the range of soil depth from 3 to 12 m, the δ^2H remained constant but exhibited fluctuations within a range of −50‰.

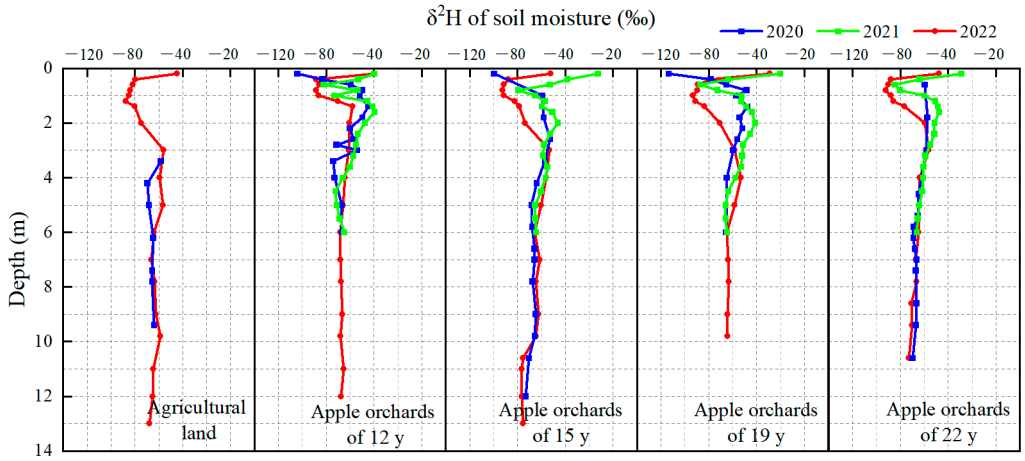


Figure 7. Distribution characteristics of δ^2H of soil moisture with depth in agricultural land and apple orchards of varying ages in 2020, 2021 and 2022.

In both 2021 and 2022, there was a decrease in the soil water δ^2H with an increasing soil depth ranging from 0–1.6 m for both agricultural land and apple orchards of varying ages. However, at depths of 1.6–3 m, there was an increase in δ^2H with an increasing soil depth for both agricultural land and apple orchards of varying ages. Values of δ^2H remained consistent at −50‰ within the range of depths from 3 to 12 m for both agricultural land and apple orchards, regardless of their age groupings. This suggests that extreme precipitation does not significantly affect the isotopic composition (δ^2H) of deep soil moisture (at depths between 3 and 12 m), allowing it to maintain its value of −50‰.

The sampling was conducted during the rainy season in 2020, resulting in surface soil moisture δ^2H being predominantly influenced by recent precipitation events. The observed δ^2H distribution curve with soil depth, exhibiting an "upper left" trend, signifies the process of isotopically depleted rainwater infiltration and subsequent mixing within the soil water.

However, the sampling was conducted during the dry seasons in 2021 and 2022, resulting in surface soil moisture δ^2H being predominantly influenced by soil evaporation. As the soil surface was approached, the intensity of evaporation increased, resulting in an 'upper-right' trend in the distribution curve of δ^2H with soil depth. Values of the δ^2H of soil moisture at depths of 1.6–3 m reflect the impact of extreme precipitation during the previous rainy season. Furthermore, in the 0–3 m soil layers, the δ^2H depth profile of the soil water in 2022 shifts to the left compared to that in 2021, indicating infiltration and mixing with isotopically depleted precipitation.

Overall, the higher δ^2H concentration in 2021 and its depletion in 2022 suggest that the extreme precipitation in 2021 replenished the soil moisture within the depth range of 0–3 m. Additionally, considering that sampling was conducted in October 2020, when it

had frequently been supplemented by rainfall from the rainy season, this led to relatively low isotope levels within the same soil layer.

The distribution of the $\delta^{18}O$ of soil moisture with a soil depth in agricultural land and apple orchards of varying ages in 2020, 2021, and 2022 is illustrated in Figure 8. It can be seen that in 2020, values of the $\delta^{18}O$ of the soil moisture of agricultural land and apple orchards of varying ages increased gradually with a soil depth of 0–3 m. After that, values of $\delta^{18}O$ of soil moisture of agricultural land and apple orchards of varying ages with soil depths of 3–12 m maintained a fluctuation near −8‰.

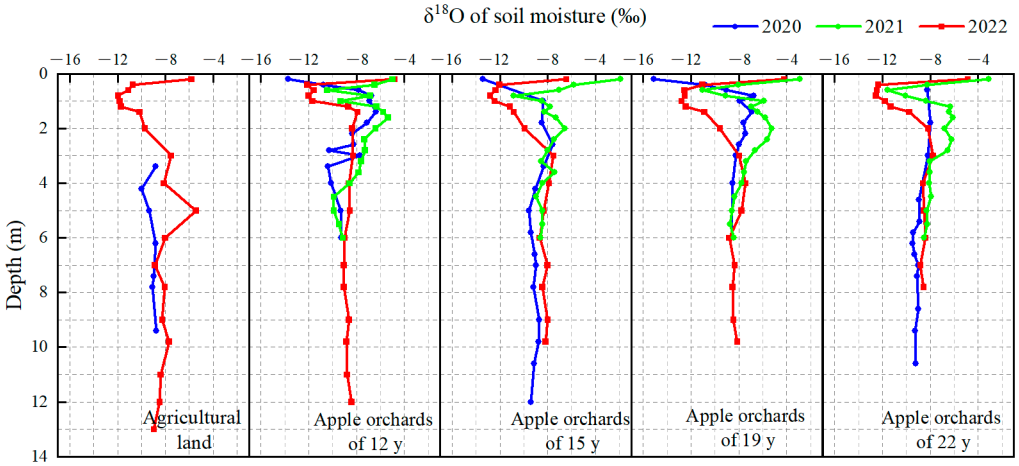


Figure 8. Distribution characteristics of soil water isotope $\delta^{18}O$ with depth in agricultural land and apple orchards of varying ages in 2020, 2021 and 2022.

In contrast, values of the $\delta^{18}O$ of soil moisture of agricultural land and apple orchards of varying ages showed a decrease with increasing soil depths of 0–3 m in 2021 and 2022. After that, values of the $\delta^{18}O$ of soil moisture of farmland and apple orchards of varying ages with a soil depth of 3–12 m maintained a fluctuation near −8‰. These findings suggest that extreme precipitation events had no significant impact on the isotopic composition ($\delta^{18}O$) of the soil moisture at depths between 3–12 m.

The isotopic composition appeared to maintain an average value close to −8‰, regardless of the extreme precipitation events. The influence of extreme precipitation events on the isotopic composition ($\delta^{18}O$) becomes evident when considering the topmost layer (0–3 m) for farmland and apple orchards. Specifically, the observations indicated an enrichment in $\delta^{18}O$ values within this layer due to intense precipitation contributions during 2021.

It should be noted that these observations were made during the October sampling, which had recently incorporated rainfall from the rainy season. Consequently, lower isotope levels were recorded within the topmost layer (0–3 m). By comparing the samples between May 2021 and May 2022, it can be inferred that the maximum infiltration depths reached approximately three meters during intense precipitation events occurring specifically in 2021.

3.2.3. Effects of Extreme Precipitation on Soil Moisture Storage and Soil Moisture Deficit in Apple Orchards of Varying Ages

The soil water storage and maximum recharge depth of farmland and apple orchards of varying ages in 2020 and 2022 are shown in Figure 9. It was evident that regardless of the year, both in 2020 and 2022, the soil water storage of apple orchards of varying ages decreased as the forest age progressed. In addition, after experiencing extreme precipitation in 2021, the soil water storage capacity of the apple orchards with varying ages in 2022 was generally higher than that in 2020, with increases of 171, 172, 442 and 290 mm, respectively. This indicated that extreme precipitation effectively replenishes the soil water storage depth from a range of depths between 4 and 10 m, but the recharge depth decreases as the age of trees increases.

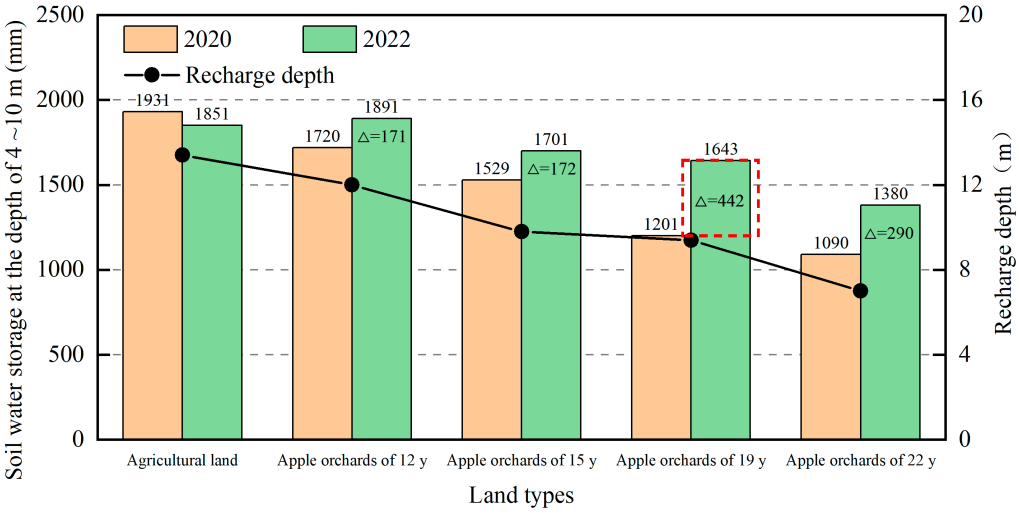


Figure 9. Maximum soil water storage and recharge depth in agricultural land and apple orchards of varying ages in 2020 and 2022.

A soil water deficit is defined as the discrepancy between soil water storage and field capacity. By employing this definition in conjunction with the local field water capacity (1739 mm), it becomes feasible to calculate the soil water deficit before and after extreme precipitation, thereby facilitating an analysis of its impact on apple orchard irrigation. Table 4 presents data on the quantity of soil water deficit and recharge in agricultural land and apple orchards of varying ages for both 2020 and 2022. It was evident that there was no water deficit observed in agricultural land prior to or following extreme precipitation events; however, a deficiency did exist within apple orchards across varying ages, with the magnitude increasing proportionally alongside forest age. Subsequent to extreme precipitation, the extent of reduction in the soil water deficit varied among apple orchards of differing ages, resulting in reductions of 19, 172, 442 and 290 mm, respectively. Notably, there was an initial increase followed by a subsequent decrease in the rate at which the soil water deficits were reduced as the age increased.

Table 4. Calculation table of soil water deficit and supplement of agricultural land and apple orchards of varying ages in 2020 and 2022.

Land Types	Year	Soil Water Storage	Field Capacity	Soil Water Deficit
		(mm)	(mm)	(mm)
Agricultural land	2020	1931	1739	0
	2022	1851	1739	0
Apple orchards of 12 y	2020	1720	1739	19
	2022	1891	1739	0
Apple orchards of 15 y	2020	1529	1739	210
	2022	1701	1739	38
Apple orchards of 19 y	2020	1201	1739	538
	2022	1643	1739	96
Apple orchards of 22 y	2020	1090	1739	649
	2022	1380	1739	359

3.3. Effects of Extreme Precipitation on Soil Recharge in Apple Orchards of Varying Ages

3.3.1. Effects of Extreme Precipitation on Soil Moisture Recharge Characteristics of Apple Orchards of Varying Ages

The variation in soil moisture consumption and recharge in agricultural land and apple orchards of varying ages with soil depth caused by extreme precipitation is illustrated in Figure 10. It can be observed that significant soil moisture consumption occurs in the soil

profiles of apple orchards at various ages following extreme precipitation events: Apple orchards of 12 y, 15 y, 19 y and 22 y had a soil water consumption of 148, 116, 100 and 86 mm at soil depths of 5.4, 5.4, 3.4 and 2.8 m, respectively; both the consumption depth and amount decreased as the age increased.

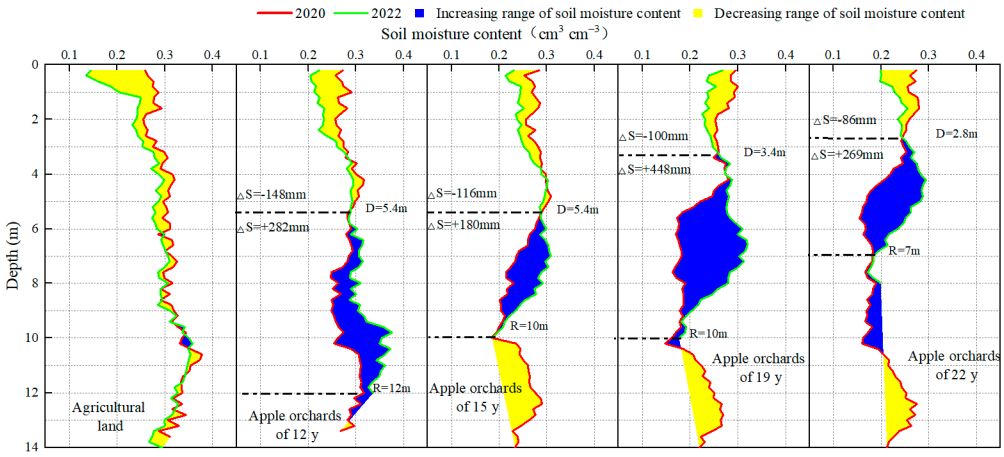


Figure 10. Differences in soil moisture content of agricultural land and apple orchards of varying ages in 2022 compared with replenishment and consumption in 2020.

Simultaneously, the soil moisture of apple orchards of varying ages was also replenished to varying degrees: the soil moisture recharge of apple orchards of 12 y, 15 y, 19 y and 22 y was 282, 180, 448 and 269 mm, and the recharge depth was 12, 10, 10 and 7 m, respectively. Moreover, the recharge depth decreased with increasing tree age. The results indicate that extreme precipitation affected the distribution of soil moisture within apple orchards differently across various depths: shallow depths exhibited a state of consumption, while deeper layers showed a state of recharge.

Table 5 presents the soil moisture recharge characteristics of agricultural land and apple orchards of varying ages. It was evident that the minimum soil moisture content prior to recharge in mature apple orchards (15 y, 19 y and 22 y) was lower than that of other lands, with values of 18%, 15%, and 16%, respectively. These values closely approached the wilting coefficient and occurred at a depth of approximately 10 m, which increased with forest age. This indicated a profound absorption and utilization of deep soil water by apple tree roots. The minimum soil moisture content before recharge in agricultural land occurs at a shallow depth (2 m), potentially due to the shallow root systems. In conjunction with Figure 9, it can be observed that the extreme precipitation recharge in 2021 would augment the soil moisture content and alleviate soil desiccation.

Table 5. Soil moisture supply characteristics of agricultural land and apple orchards of varying ages.

Land Types	Minimum Soil Moisture Content Before Recharge (%)	Depth of Minimum Soil Moisture Content Before Recharge (mm)	Maximum Soil Moisture Content After Recharge (%)	Depth of Maximum Soil Moisture Content Before Recharge (mm)
Agricultural land	25	2	36	10.2
Apple orchards of 12 y	25	7.8	38	9.8
Apple orchards of 15 y	18	9.8	31	7
Apple orchards of 19 y	15	10	32	6.6
Apple orchards of 22 y	16	10.2	29	4.2

Furthermore, following extreme precipitation recharge, a maximum soil moisture content was observed in agricultural land and apple orchards of 12 y, being 36 and 38%, respectively, occurring at depths exceeding field capacity (approximately 10 m), facilitating soil water transport. Conversely, the maximum soil moisture content for mature apple

orchards was slightly lower and occurred at shallower depths (ranging from 4.2 to 7 m). The larger soil water deficit in aged apple orchards may account for the challenge of achieving deep infiltration after a certain amount of precipitation had replenished the upper soil layers.

3.3.2. Effects of Extreme Precipitation on Soil Water Recharge Depth in Apple Orchards of Varying Ages

The tritium concentration variation with soil depth in agricultural land and apple orchards of varying ages in 2020 and 2022 is illustrated using scatter plots, as shown in Figure 11. It was evident that the tritium profile displays varying degrees of horizontal displacement following extreme precipitation events: the tritium profile in soil moisture within agricultural land shifted to the right, while the tritium profile in apple orchards shifted to the left. This displacement change was associated with the soil moisture content. Due to a relatively stable total amount of tritium in the soil, the soil moisture content corresponding to the tritium peak decreased after extreme precipitation, resulting in a concentration effect on the tritium concentration within agricultural land. Consequently, this caused a rightward shift in the tritium profile of soil moisture within agricultural land. Conversely, after experiencing similar extreme precipitation events, there was an increase in the soil moisture content corresponding to the tritium peak within apple orchards, leading to a dilution effect on their tritium concentration. As a result, there was an observed leftward shift in the tritium profile within the apple orchard's soil water.

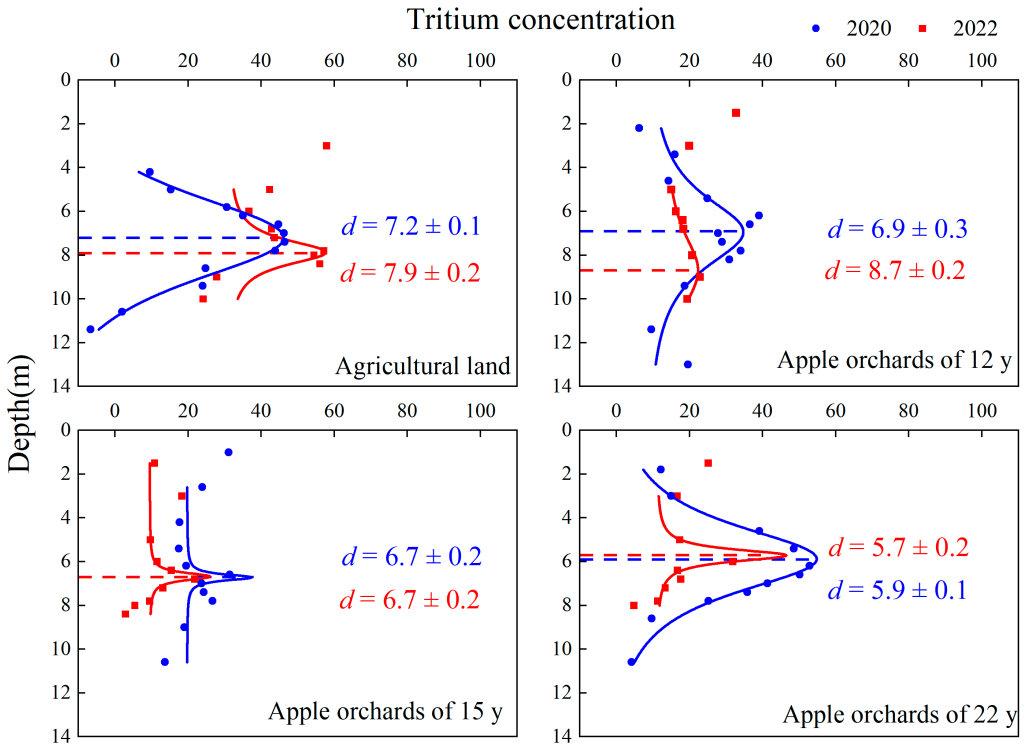


Figure 11. Distribution characteristics of soil water tritium peak with depth in agricultural land and apple orchards of varying ages in 2020 and 2022.

Additionally, the solute dispersion convection equation was utilized to fit the soil depths corresponding to the tritium peak in agricultural land and apple orchards of varying ages in 2020 and 2022. In 2020, the measured soil depths for the agricultural land and apple orchards of 12 y, 15 y and 22 y were recorded as follows: 7.2, 6.9, 6.7 and 5.7 mm, respectively, whereas in 2022, they were observed as: 7.9, 8.7, 6.7 and 5.9 mm. It was noted that compared to the agricultural land across varying age groups of trees, the soil

depth associated with the tritium peak concentration tended to be lower in apple orchards, indicating a potential inhibition of soil moisture transport due to apple tree cultivation.

The comparison of soil depth corresponding to the tritium peak in agricultural land and apple orchards of varying ages before and after extreme precipitation revealed a decrease in peak values for both land types, with migration distances measuring 0.7, 1.8, 0 and 0.2 mm, respectively. Notably, in the apple orchard of 12 y, the migration distance of the tritium peak was the largest, and after extreme precipitation, its depth exceeded that observed in agricultural land.

3.3.3. Effects of Extreme Precipitation on Soil Moisture Recharge Modes in Apple Orchards of Varying Ages

According to the definition, the lc-excess of precipitation isotopes is 0‰, indicating an absence of evaporation. The value of the lc-excess of the soil sample after evaporation typically exhibits negative values, with a lower negative value indicating more pronounced evaporation characteristics [36]. Therefore, by calculating the values of vertical lc-excess in the soil profile and analyzing their changes, alternating patterns of precipitation infiltration and soil evaporation can be examined. The results are depicted in Figure 12.

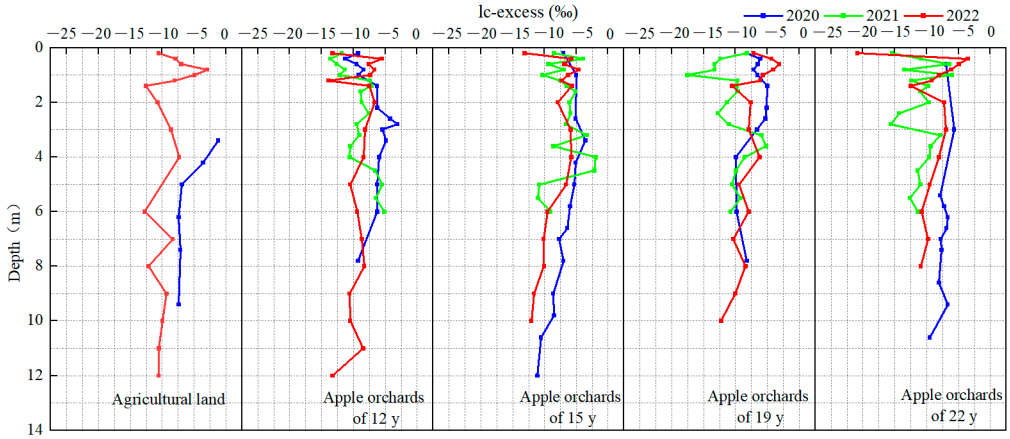


Figure 12. Distribution characteristics of soil water lc-excess with depth in agricultural land and apple orchards of varying ages in 2020, 2021 and 2022.

Regardless of before or after extreme precipitation events, the lc-excess of the soil moisture in agricultural land and apple orchards remained below 0, indicating significant soil evaporation. Additionally, it can be observed that shallow soil exhibits substantial fluctuations in lc-excess, while deep soil experiences minimal variations. This phenomenon arises from the surface layer's susceptibility to both evaporation-induced reduction during dry seasons and a precipitation-induced increase during rainy seasons, resulting in sharp changes in the lc-excess at this depth. However, below a certain depth (4 m), where the influence of precipitation and evaporation diminished, the lc-excess signal tended to stabilize and was solely affected by soil moisture infiltration.

From the perspective of year, the Lc-excess of the soil moisture in October 2020 exhibited a greater magnitude compared to that observed in May 2021 and May 2022, potentially attributed to the lower temperatures and recented rainy season during sampling in October 2020. These conditions suppressed the evaporation intensity, consequently resulting in a higher lc-excess value. Conversely, as May 2021 and May 2022 approached summer with increased temperatures, intensified soil evaporation contributed to a reduction in lc-excess.

From the perspective of land types, taking the sampled soil profile in May 2022 as an example, the minimum values of the soil moisture lc-excess were observed at a depth of 0.2 m in agricultural land and apple orchards of varying ages. Conversely, the maximum values appeared at a depth of 0.4 m in these land types. Values of the lc-excess of the soil moisture exhibited alternating patterns between minimum and maximum

levels, accompanied by a decreasing fluctuation range. In apple orchards of 19 y and 22 y, deeper soil layers demonstrated greater stability in the lc-excess values due to the long-term depletion of soil water, resulting in the formation of a dry layer that may impede preferential flow occurrence. Consequently, the piston flow was considered the predominant mode for recharging soil water, leading to minimal fluctuations in the lc-excess value.

4. Discussion

4.1. The Impact of Extreme Precipitation on Soil Moisture Distribution at Varying Growth Stages in Apple Orchards

The distribution of soil moisture is influenced by various factors, including land use, microtopography, the physical and chemical properties of the soil, as well as precipitation. These factors collectively contribute to intricate and dynamic changes in the soil moisture content [37]. However, precipitation plays a pivotal role as the primary determinant of soil water content [38]. In general, increased precipitation leads to an increase in soil moisture content. Specifically, a shallow soil moisture content above 10 cm is significantly influenced by rainfall [39]. Shallow soil moisture content experiences a substantial increase following the onset of precipitation. Deep soil moisture content is affected by the piston flow and takes some time to respond [40]. Therefore, it can be inferred that deep soil moisture reflects past precipitation. Based on Figure 5, it is evident that the deep soil moisture content in apple orchards of varying ages in 2022 surpasses that of both 2020 and 2021. This observation signifies a replenishment of soil moisture subsequent to the extreme precipitation encountered in 2021, aligning with previous research findings [7,33,41]. However, the depth at which the soil moisture content exceeds that of 2020 is influenced by orchard ages: following extreme precipitation events, the initial depths where the soil moisture content increases are observed to decrease as orchard ages advance (at depths of 5.4 m for 12 y orchard, 4.2 m for 15 y orchard, 3.4 m for 19 y orchard and 2.8 m for 22 y orchard). This phenomenon may be attributed to an augmentation in root extension with tree age, facilitating preferential flow activity and enhancing subsurface water infiltration.

The stable isotopic values in shallow soil moisture exhibit variations influenced by both evaporation and mixing processes [14]. Conversely, the changes in deep soil moisture isotopics primarily result from mixing processes [42]. Therefore, comparing the precipitation changes with stable isotopic composition alterations can provide valuable insights into understanding the mechanisms governing soil water movement. By comparing the δ^2H values of soil samples collected in May 2021 and May 2022, it is evident that extreme precipitation leads to a depletion of δ^2H at depths of 0–3 m. As we delve deeper into the soil profile, the difference in δ^2H between pre- and post-extreme rainfall gradually diminishes until reaching equilibrium at approximately 3 m. Subsequently, there is an enrichment of δ^2H within the depth range of 3–6 m after extreme precipitation, followed by another equilibrium point around 6 m. From these observations, it can be concluded that during piston flow recharge, resulting from extreme precipitation in 2021, the maximum infiltration depth was approximately 3 m, while soil moisture movement occurred below this level. The fluctuation in δ^2H observed at a depth of 12 m indicates a preferential flow replenishing the soil water content within this layer in the apple orchard of 15 y. Conversely, minimal variations exist in the δ^2H values below 3 m within the apple orchard of 22 y. Taking into account these findings along with the status of soil moisture, it can be inferred that significant evapotranspiration rates have led to the development of a dry layer within the topsoil profile of the apple orchard of 12 y. This dry layer rapidly absorbs incoming water and impedes preferential flow generation.

4.2. Effects of Extreme Precipitation on Soil Moisture Recharge at Varying Growth Stages in Apple Orchards

Differences in the transport distance of tritium peaks between farmland and apple orchards with varying forest ages suggest a potential correlation with the soil moisture content at the specific depth where the tritium peak is located. Tritium peaks in the apple orchard at 12 y exhibit the maximum migration distance, followed by farmland, and the

tritium peaks at 15 y and 22 y show minimal movement. Considering the soil moisture content, it can be inferred that extreme precipitation leads to an excess of soil moisture in the depth range of 6–12 m within the 12 y apple orchard, surpassing its field water-holding capacity, and particularly within the depth range of 9.5–11 m, the soil moisture content exceeds 0.35 m^3 m^{-3}. Based on wetting front migration patterns during water infiltration processes, it can be concluded that a high soil moisture content (0.35 m^3 m^{-3}) has been transferred through water movements at depths where tritium peaks are located in the 12 y orchard. Under these conditions, effective water transport facilitates the downward migration of tritium peaks.

Other apple orchards display a maximum soil moisture content of around 0.30 m^3 m^{-3} after replenishment and do not exhibit a similar zone with enhanced moisture transmission, as observed in the 12 y orchard. Although the agricultural land shows a relatively high soil moisture content at a depth of 10.8 m due to extreme precipitation events before and after—which resulted in similar shapes for the soil moisture curves—it is believed that extreme precipitation may not have significantly altered the stable soil moisture transport status in farmland during this process since the soil moisture at depths where tritium peaks are located remains around 0.30 m^3 m^{-3} (without effectively promoting the downward migration of tritium peaks occurring). Therefore, it can be speculated that the formation of a zone with higher (greater than 0.35 m^3 m^{-3}) soil moisture content at the depths where tritium peaks are located is necessary to effectively promote their migration.

5. Conclusions

This study takes Changwu Yuan, a representative apple planting area on the Loess Plateau, as a case study to comprehensively investigate the impact of extreme precipitation on soil water movement based on indicators such as the soil water storage capacity and the recharge rate depth. The main findings are as follows:

(1) Extreme precipitation has a mitigating effect on soil dryness by replenishing soil moisture in apple orchards. However, the depth of water supply decreases with the increasing age of apple trees. (2) The longitudinal distribution of soil moisture content exhibits an overall trend toward deeper layers, indicating the downward movement of soil moisture in the presence of a piston flow as the dominant mode of water transport. (3) Following extreme precipitation events, both farmland and apple orchards show a downward shift in the tritium peak; substantial rainfall is required to establish a high-moisture transfer zone (greater than 0.35 m^3 m^{-3}) at the depth corresponding to the tritium peak for effective tritium migration. (4) The lc-excess values for farmland and apple orchards fluctuate within a certain range (10‰) with increasing depth; the piston flow is identified as the primary mechanism governing soil water movement, while changes in the lc-excess at deeper layers indicate a preferential flow as an additional supply mechanism.

Author Contributions: Conceptualization, J.H. and Y.H.; methodology, J.H., Y.H. and H.W.; software, J.H. and Y.H.; validation, J.H. and Y.H.; formal analysis, J.H. and Y.H.; investigation, J.H. and Y.H.; resources, J.H. and Y.H.; data curation, J.H. and Y.H.; writing—original draft preparation, J.H. and H.W.; writing—review and editing, W.X., L.G. and Y.T.; visualization, J.H. and Y.Z.; supervision, Q.L.; project administration, Y.W. and M.L.; funding acquisition, Y.W. and M.L. All authors have read and agreed to the published version of the manuscript.

Funding: This study was financially supported by the National Key R&D Program of China (2022YEE0100300), the National Natural Science Foundation of China (52479051), and the Sichuan Program of Science and Technology (2023JDZH0010, 2024NSFSC0126).

Data Availability Statement: The raw data supporting the conclusions of this article will be made available by the authors upon request.

Conflicts of Interest: The authors declare no conflict of interest.

References

1. Lemoine, N.P.; Budny, M.L. Seasonal soil moisture variability, not drought, drives differences in photosynthetic physiology of two C4 grass species. *Plant Ecol.* **2022**, *223*, 627–642. [CrossRef]
2. Shao, R.; Jia, S.; Tang, Y.; Zhang, J.; Li, H.; Li, L.; Chen, J.; Guo, J.; Wang, H.; Yang, Q.; et al. Soil water deficit suppresses development of maize ear by altering metabolism and photosynthesis. *Environ. Exp. Bot.* **2021**, *192*, 104651. [CrossRef]
3. Zhao, C.; Jia, X.; Zhu, Y.; Shao, M. Long-term temporal variations of soil water content under different vegetation types in the Loess Plateau, China. *CATENA* **2017**, *158*, 55–62. [CrossRef]
4. Huang, Y.; Chang, Q.; Li, Z. Land use change impacts on the amount and quality of recharge water in the loess tablelands of China. *Sci. Total Environ.* **2018**, *628–629*, 443–452. [CrossRef] [PubMed]
5. Zhang, Q.; Fan, J.; Zhang, S.; Zhao, X.; Luo, Z.; Zhou, G. Changes and driving factors of soil water in mixed-species plantations and different precipitation scenarios on the Loess Plateau of China. *CATENA* **2024**, *246*, 108370. [CrossRef]
6. Bao, H.; Tang, M.; Lan, H.-X.; Peng, J.-B.; Zheng, H.; Guo, G.-M. Soil erosion and its causes in high-filling body: A case study of a valley area on the Loess Plateau, China. *J. Mt. Sci.* **2023**, *20*, 182–196. [CrossRef]
7. Li, T.; Shao, M.; Jia, Y.; Jia, X.; Huang, L. Profile distribution of soil moisture in the gully on the northern Loess Plateau, China. *CATENA* **2018**, *171*, 460–468. [CrossRef]
8. Wen, Y.; Li, M.; Xu, R.; Qiu, D.; Gao, P.; Mu, X. Spatial distribution characteristics and influencing factors of shallow and deep soil moisture under ecological restoration in the loess plateau, China. *Hydrol. Process.* **2024**, *38*, e15109. [CrossRef]
9. Chen, Y.; Qian, H.; Hou, K.; Zhang, Q.; Zhang, Y. Vertical distribution characteristics of soil moisture with different strata in deep profile in Guanzhong Basin, China. *Environ. Earth Sci.* **2020**, *79*, 103. [CrossRef]
10. He, Z.; Jia, G.; Liu, Z.; Zhang, Z.; Yu, X.; Xiao, P. Field studies on the influence of rainfall intensity, vegetation cover and slope length on soil moisture infiltration on typical watersheds of the Loess Plateau, China. *Hydrol. Process.* **2020**, *34*, 4904–4919. [CrossRef]
11. Xu, G.; Huang, M.; Li, P.; Li, Z.; Wang, Y. Effects of land use on spatial and temporal distribution of soil moisture within profiles. *Environ. Earth Sci.* **2021**, *80*, 128. [CrossRef]
12. Han, J.-J.; Duan, X.; Zhao, Y.-Y.; Li, M. Characteristics of Stable Hydrogen and Oxygen Isotopes of Soil Moisture under Different Land Use in Dry Hot Valley of Yuanmou. *Open Chem.* **2019**, *17*, 105–115. [CrossRef]
13. Rau, G.C.; Andersen, M.S.; McCallum, A.M.; Acworth, R.I. Analytical methods that use natural heat as a tracer to quantify surface water–groundwater exchange, evaluated using field temperature records. *Hydrogeol. J.* **2010**, *18*, 1093–1110. [CrossRef]
14. Du, K.; Zhang, B.; Li, L. Soil Water Dynamics Under Different Land Uses in Loess Hilly Region in China by Stable Isotopic Tracing. *Water* **2021**, *13*, 242. [CrossRef]
15. Zheng, W.; Wang, S.; Sprenger, M.; Liu, B.; Cao, J. Response of soil water movement and groundwater recharge to extreme precipitation in a headwater catchment in the North China Plain. *J. Hydrol.* **2019**, *576*, 466–477. [CrossRef]
16. Liu, W.; Zhang, X.-C.; Dang, T.; Ouyang, Z.; Li, Z.; Wang, J.; Wang, R.; Gao, C. Soil water dynamics and deep soil recharge in a record wet year in the southern Loess Plateau of China. *Agric. Water Manag.* **2010**, *97*, 1133–1138. [CrossRef]
17. Huang, Y.; Evaristo, J.; Li, Z. Multiple tracers reveal different groundwater recharge mechanisms in deep loess deposits. *Geoderma* **2019**, *353*, 204–212. [CrossRef]
18. Sun, J.; Li, B.; Wang, W.; Yan, X.; Li, Q.; Li, Z. Variations and controls on groundwater recharge estimated by combining the water-table fluctuation method and Darcy's law in a loess tableland in China. *Hydrogeol. J.* **2024**, *32*, 379–394. [CrossRef]
19. Song, X.; Wang, S.; Xiao, G.; Wang, Z.; Liu, X.; Wang, P. A study of soil water movement combining soil water potential with stable isotopes at two sites of shallow groundwater areas in the North China Plain. *Hydrol. Process.* **2009**, *23*, 1376–1388. [CrossRef]
20. Zhu, X.; He, Z.-B.; Du, J.; Chen, L.-F.; Lin, P.-F.; Li, J. Temporal variability in soil moisture after thinning in semi-arid Picea crassifolia plantations in northwestern China. *For. Ecol. Manag.* **2017**, *401*, 273–285. [CrossRef]
21. Luan, J.; Zhang, Y.; Li, X.; Ma, N.; Naeem, S.; Xu, Z.; He, S.; Miao, P.; Tian, X.; Wang, R. Unexpected consequences of large-scale ecological restoration: Groundwater declines are reversed. *Ecol. Indic.* **2023**, *155*, 111008. [CrossRef]
22. Ye, S.; Li, J.; Kong, H.; Shen, J.; Wu, D. Effects of different mulch materials on the photosynthetic characteristics, yield, and soil water use efficiency of wheat in Loess tableland. *Sci. Rep.* **2023**, *13*, 18106. [CrossRef] [PubMed]
23. Li, W.; Gao, J.; Zhang, Y.; Ahmad, R.; Gao, Z.; Zhou, F. Effects of Planting Practices on Soil Organic Carbon during Old Apple Orchards' Reconstruction on the Loess Plateau. *Agronomy* **2023**, *13*, 897. [CrossRef]
24. Lu, Y.; Li, H.; Si, B.; Li, M. Chloride tracer of the loess unsaturated zone under sub-humid region: A potential proxy recording high-resolution hydroclimate. *Sci. Total Environ.* **2020**, *700*, 134465. [CrossRef] [PubMed]
25. Houborg, R.; McCabe, M.F. Adapting a regularized canopy reflectance model (REGFLEC) for the retrieval challenges of dryland agricultural systems. *Remote Sens. Environ.* **2016**, *186*, 105–120. [CrossRef]
26. Zhang, B.; Huang, J.; Dai, T.; Jing, S.; Hua, Y.; Zhang, Q.; Liu, H.; Wu, Y.; Zhang, Z.; Chen, J. Assessing accuracy of crop water stress inversion of soil water content all day long. *Precis. Agric.* **2024**, *25*, 1894–1914. [CrossRef]
27. Igaz, D.; Aydin, E.; Šinkovičová, M.; Šimanský, V.; Tall, A.; Horák, J. Laser Diffraction as An Innovative Alternative to Standard Pipette Method for Determination of Soil Texture Classes in Central Europe. *Water* **2020**, *12*, 1232. [CrossRef]
28. Huang, J.; Wang, S.; Guo, Y.; Chen, J.; Yao, Y.; Chen, D.; Liu, Q.; Zhang, Y.; Zhang, Z.; Xiang, Y. Hysteresis between winter wheat canopy temperature and atmospheric temperature and its driving factors. *Plant Soil* **2024**, *499*, 55–71. [CrossRef]

29. Tao, G.; Lei, D.; Liu, L.; Li, Y.; Zhu, X. Prediction of Soil Water Characteristic Curve Based on Soil Water Evaporation. *Adv. Civ. Eng.* **2021**, *2021*, 6686442. [CrossRef]
30. Sprenger, M.; Tetzlaff, D.; Tunaley, C.; Dick, J.; Soulsby, C. Evaporation fractionation in a peatland drainage network affects stream water isotope composition. *Water Resour. Res.* **2017**, *53*, 851–866. [CrossRef]
31. Huang, T.; Ma, B.; Pang, Z.; Li, Z.; Li, Z.; Long, Y. How does precipitation recharge groundwater in loess aquifers? Evidence from multiple environmental tracers. *J. Hydrol.* **2020**, *583*, 124532. [CrossRef]
32. Mathias, S.A.; Butler, A.P.; McIntyre, N.; Wheater, H.S. The significance of flow in the matrix of the Chalk unsaturated zone. *J. Hydrol.* **2005**, *310*, 62–77. [CrossRef]
33. Shi, P.; Huang, Y.; Ji, W.; Xiang, W.; Evaristo, J.; Li, Z. Impacts of deep-rooted fruit trees on recharge of deep soil water using stable and radioactive isotopes. *Agric. For. Meteorol.* **2021**, *300*, 108325. [CrossRef]
34. Chen, K.; Liu, G.; Xia, C.; Meng, Y.; Tetzlaff, D.; Zhong, Q.; Chang, J. Water cycling and partitioning through the soil–plant–atmosphere continuum in a subtropical, urban woodland inferred by water stable isotopes. *Hydrol. Process.* **2022**, *36*, e14746. [CrossRef]
35. Sprenger, M.; Tetzlaff, D.; Soulsby, C. Soil water stable isotopes reveal evaporation dynamics at the soil–plant–atmosphere interface of the critical zone. *Hydrol. Earth Syst. Sci.* **2017**, *21*, 3839–3858. [CrossRef]
36. Landwehr, J.M.; Coplen, T.B.; Stewart, D.W. Spatial, seasonal, and source variability in the stable oxygen and hydrogen isotopic composition of tap waters throughout the USA. *Hydrol. Process.* **2014**, *28*, 5382–5422. [CrossRef]
37. Souza Wojahn, V.d.; Bartels, G.K.; Collares, G.L. Temporal stability of soil moisture: A case study in a small watershed in the subtropical region of Brazil. *Environ. Earth Sci.* **2023**, *82*, 61. [CrossRef]
38. Gierke, C.; Newton, B.T.; Phillips, F.M. Soil-water dynamics and tree water uptake in the Sacramento Mountains of New Mexico (USA): A stable isotope study. *Hydrogeol. J.* **2016**, *24*, 805–818. [CrossRef]
39. Zhu, S.; Li, H.; Xu, W.; Zhang, T.; Liu, C.; Peng, Y. Dynamic process and model simulation of soil water content during citrus growth period. *Acta Geophys.* **2023**, *71*, 1525–1537. [CrossRef]
40. Pu, H.; Song, W.; Wu, J. Using Soil Water Stable Isotopes to Investigate Soil Water Movement in a Water Conservation Forest in Hani Terrace. *Water* **2020**, *12*, 3520. [CrossRef]
41. Xiang, W.; Si, B.C.; Biswas, A.; Li, Z. Quantifying dual recharge mechanisms in deep unsaturated zone of Chinese Loess Plateau using stable isotopes. *Geoderma* **2019**, *337*, 773–781. [CrossRef]
42. Zhou, J.J.; Wang, X.; Ma, L.; Luo, C.Y.; Tang, H.T.; Guo, Z.N.; Chen, J.W.; Shi, S.H.; Shi, W.; Wei, W.; et al. Variation of soil-plant-atmosphere continuum stable isotope and water source in Qinghai spruce forest of the eastern Qilian Mountains. *J. Mt. Sci.* **2023**, *20*, 355–366. [CrossRef]

Disclaimer/Publisher's Note: The statements, opinions and data contained in all publications are solely those of the individual author(s) and contributor(s) and not of MDPI and/or the editor(s). MDPI and/or the editor(s) disclaim responsibility for any injury to people or property resulting from any ideas, methods, instructions or products referred to in the content.